IBRO Reports 4 (2018) 1–6

Contents lists available at ScienceDirect

IBRO Reports

journal homepage: http://www.journals.elsevier.com/ibro-reports

Neonatal spinal injury induces de novo projections of primary afferents to the lumbosacral intermediolateral nucleus in rats

Masahito Takiguchi, Mai Fujioka, Kengo Funakoshi *

Department of Neuroanatomy, Yokohama City University School of Medicine, 3-9 Fukuura, Kanazawa-ku, Yokohama, 236-0004, Japan

ARTICLE INFO

Article history:
Received 24 March 2017
Received in revised form
24 November 2017
Accepted 28 November 2017

ABSTRACT

Complete spinal transection in adult rats results in poor recovery of hind limb function and severe urinary bladder dysfunction. Neonatal rats with spinal cord transection, however, exhibit spontaneous and significant recovery of micturition control. A previous study in which biotinylated-dextran amine (BDA) was used as an anterograde tracer demonstrated that primary afferent fibers from the fifth lumbar dorsal root ganglion (DRG) project more strongly and make more terminals in the ventral horn after neonatal spinal cord transection at the mid-thoracic level. In the present study, we injected BDA into the sixth lumbar (L6) DRG of neonatally spinalized rats to label primary afferent fibers that include visceral afferents. The labeled fibers projected to the intermediolateral nucleus (IML) in the intermediate zone on ipsilateral side of the L6 spinal segment, whereas no projections to the IML were observed in sham-operated or intact rats. The BDA-labeled fibers of neonatally spinalized rats formed varicose terminals on parasympathetic preganglionic neurons in the IML. These findings suggest that some primary afferent projections from the L6 DRG to the IML appear after neonatal spinal cord transection, and these de novo projections might contribute to the recovery of autonomic function such as micturition following spinal cord injury in the neonatal stage.

1. Introduction

Spinal cord injury (SCI) in the adult causes sensorimotor and autonomic dysfunction, even leading to death in some cases (Krassioukov et al., 2007). Despite numerous studies aimed at enhancing recovery from impairments caused by SCI, no therapeutic strategies for SCI have been established (Mathias and Low, 2014). In experimental studies, thoracic spinal cord transection in adult rats and cats leads to severe bladder dysfunction in addition to paraplegia at spinal levels below the injury site (de Groat et al., 1998). Severe dysuria in rodents with complete SCI is usually managed by researchers manually pressing on the urinary bladder twice a day (Herrera et al., 2010).

Rats that undergo spinal cord transection at the neonatal period, however, exhibit far less motor dysfunction compared to those at the adult stage (Stelzner et al., 1975; Yuan et al., 2013; Takiguchi et al., 2015). We recently demonstrated that compensatory projections of primary afferent fibers to the intermediate zone and the ventral horn in the lumbar spinal segment are strengthened after neonatal spinal cord transection at the thoracic level, based on experiments in which biotinylated dextran amine (BDA), an anterograde tracer, was administered into the dorsal root ganglion (DRG) (Takiguchi et al., 2015). This plastic change in the primary afferent projections caused by neonatal spinal cord transection might be involved in the ameliorative effects on motor function because axonal regeneration of descending tracts through the injury site has not been confirmed in either the neonatal SCI model or the adult SCI model.

In contrast to motor function, the mechanisms underlying the recovery of autonomic function after neonatal SCI have not been thoroughly investigated. In adult rats, several brain regions are important for controlling micturition. Among them, the pontine micturition center, also referred to as Barrington's nucleus, is considered mainly responsible for regulating micturition (de Groat et al., 1998). The descending projections from Barrington's nucleus to the lumbosacral spinal cord form by postnatal day (P5) in neonatal rats (Sugaya et al., 1997). When supraspinal projections from the pontine micturition center are interrupted in neonatal rats, primary afferent projections to the spinal cord may increase to compensate for urinary bladder dysfunction. In the present study, therefore, we examined whether primary afferent projections to the intermediolateral nucleus (IML) in the sixth lumbar (L6) spinal

* Corresponding author.
E-mail address: funako@med.yokohama-cu.ac.jp (K. Funakoshi).

https://doi.org/10.1016/j.ibror.2017.11.002

segment, which contains parasympathetic preganglionic neurons (PPNs), are increased in neonatally spinalized rats. We labeled primary afferent fibers by administering BDA into the L6 DRG, which contains visceral afferents from the urinary bladder. We then examined chemical markers of DRG neurons incorporating the BDA using double-labeling immunohistochemistry.

2. Materials and methods

2.1. Materials

Wistar rats neonates (n = 45, Japan SLC, Hamamatsu, Japan) and Wistar rat dams (n = 4, Japan SLC) were used in the present study. All experimental procedures were performed according to the standards established by the NIH Health Guide for the Care and Use of Laboratory Animals and the Policies on the Use of Animals and Humans in Research. The protocols were approved by the Institutional Animal Care and Use Committee of the Animal Research Center, Yokohama City University Graduate School of Medicine.

2.2. Neonatal spinal cord transections

The spinal cords of P5 rat pups (n = 13; neo-ST rats) that were randomly selected from each four litters were completely transected at the eighth thoracic (T8) level, as previously described (Takiguchi et al., 2015). Briefly, under anesthesia with isoflurane gas (1.0%-2.0%), spinal cords were completely transected with small spring microscissors following partial laminectomy (T7-T9). Once bleeding stopped, the muscles, fascia, and skin were closed in layers using 6-0 nylon sutures. The rats were gently cleaned with gauze soaked in 70% ethanol to eliminate the smell of blood, then returned to their home cages after recovery from anesthesia. Sham-operated rats (n = 13) from four litters underwent laminectomy, but no spinal transection. Intact rats (n = 19) from four litters underwent no surgical treatments. These three groups were randomly allocated in almost equal proportions from each litter. All rat pups were returned to their dams. All rat pups were weaned at 3 weeks after surgery (P26) and housed individually in polycarbonate cages in a room maintained at 25 ± 1 °C, with a 05:00 on/19:00 off light cycle. Neo-ST rats exhibited severe motor disturbances of the hind limbs, but they could sweep their limbs by extensively moving their joints. They could also urinate by themselves.

2.3. BDA administration

At P33, BDA was administered into the L6 DRG to label primary afferent fibers by a protocol similar to that reported previously (Takiguchi et al., 2015). All rats (n = 45) were anesthetized with isoflurane and the left L6 DRG was exposed following unilateral laminectomy. BDA (0.5 μL; MW 10 kDa, 10% in distilled water, D1956, Life Technologies, Carlsbad, CA, USA) was injected using a glass pipette attached to a micromanipulator (MNM-333, Narishige, Tokyo, Japan). The tip of the pipette was 50 μm in diameter, and the micropipette was connected to a 1.0-μL Hamilton syringe by polyethylene tubing (size 5, Igarashi Ika Kogyo Co., Ltd., Tokyo, Japan). After the injection, the muscles, fascia, and skin were sutured in layers using 4-0 nylon.

2.4. Tissue preparation

Tissue processing was performed according to a modified protocol as previously described (Takiguchi et al., 2015). One week after the BDA injection, the rats were deeply anesthetized with isoflurane and transcardially perfused with 4% paraformaldehyde (4% PFA) in 0.1 M phosphate buffer (PB). The spinal cord and L6 DRG were dissected and postfixed with 4% PFA overnight at 4 °C. The tissues were cryoprotected in 25% sucrose in 0.1 M PB for 2 days and embedded in O.C.T. compound by immersion in 2-methylbutane (isopentane) cooled by liquid N_2. Sections of the DRGs and spinal cords including the L6 segment were cut at a thickness of 50 μm with a cryostat (CM3050 S, Leica, Nussloch, Germany) and stored in 0.01 M phosphate-buffered saline (PBS) at 4 °C. To visualize DRG immunofluorescence, 20-μm thick sections were cut using the same cryostat and mounted on gelatin-coated microscope slides.

2.5. BDA histochemistry

Some serial sections of the spinal cord were used for BDA histochemistry. BDA was visualized with a Vectastain Elite ABC standard kit (PK-6100, Vector Laboratories, Inc., Burlingame, CA, USA). The nickel-enhanced method was used as previously described (Takiguchi et al., 2015).

2.6. Double-labeling Immunohistochemistry

Some serial sections of the L6 spinal segment were mounted on microscope slides. The sections were post-fixed in 4% PFA in 0.1 M PB (pH 7.4) for 15 min at room temperature. After rinsing in 25 mM PBS, the sections were incubated in PBS containing 0.1% Tween 20 (PBST) for 30 min. The sections were then washed in PBS and placed in blocking solution, 5% (w/v) Block Ace (Dainippon Pharmaceutical Co., Ltd., Tokyo, Japan) at room temperature for 60 min. Following the blocking procedure, the spinal cord sections were incubated with goat polyclonal anti-choline acetyl transferase (ChAT; 1:100, Millipore, Temecula CA, USA) overnight at 4 °C. The next day, the sections were rinsed in PBST and PBS, and subsequently incubated for 90 min at room temperature in DyLight 488-conjugated donkey anti-goat IgG (H + L) (1:400, 705-485-147, Jackson ImmunoResearch Laboratories, West Grove, PA, USA) After several washes, the sections were incubated with Alexa Fluor 555-conjugated streptavidin (1:150, S32355, Life Technologies). The slides were coverslipped with slow-fade reagent (SlowFade Gold antifade reagent, S36936, Invitrogen, Carlsbad, CA, USA).

Cryosections of the DRGs on the slides were post-fixed in 4% PFA in 0.1 M PB (pH 7.4) for 15 min at room temperature. After rinsing in 25 mM PBS, the sections were incubated in PBST for 30 min. Next, the sections were washed in PBS and placed in blocking solution at room temperature for 60 min. Following the blocking procedure, the sections were incubated with goat polyclonal anti-calcitonin gene-related peptide (CGRP; 1:200, 1720–9007, AbD Serotec, Kidlington, UK), or mouse monoclonal anti-neurofilament 200 kDa (RT-97; 1:200, GeneTex Inc., Irvine, CA, USA) overnight at 4 °C. The next day, the sections were rinsed in PBST and PBS, and subsequently incubated for 90 min at room temperature in DyLight 488-conjugated donkey anti-goat IgG (H + L) (1:400, 705-485-147, Jackson ImmunoResearch Laboratories) or DyLight 488-conjugated donkey anti-mouse IgG (H + L) (1:400, 715-485-150, Jackson ImmunoResearch Laboratories). After several washes, the sections were incubated with Alexa Fluor 555-cojugated streptavidin (1:150, S32355, Life Technologies). The slides were coverslipped with slow-fade reagent (SlowFade Gold antifade reagent, S36936, Invitrogen).

The specificity of the antibodies was verified by incubation with 0.5% normal mouse serum (Jackson ImmunoResearch Laboratories), or 0.5% normal goat serum (Jackson Immuno Research Laboratories) instead of the primary antibodies.

2.7. Image acquisition and analysis

Z-stack Images of the DRG and spinal cord were digitally photographed using a Keyence BIOREVO microscope (BZ-9000,

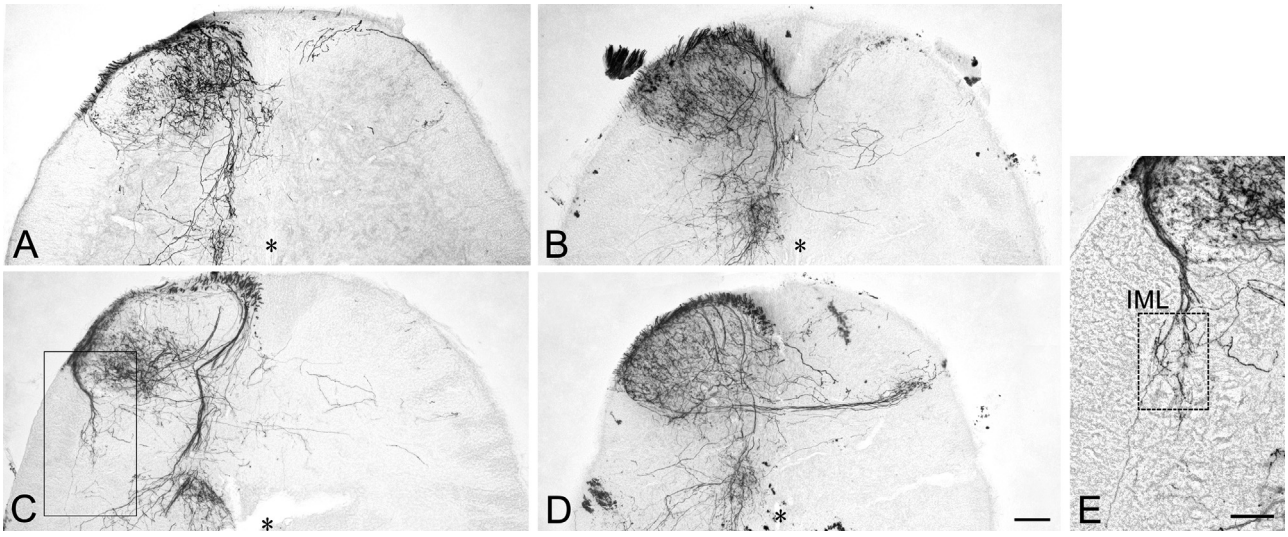

Fig. 1. Nickel-enhanced BDA staining for the L6 spinal cord segment. **A–D:** Low-magnification z-stack images of the dorsal spinal cord of intact rats (**A**), sham-operated rats (**B**), and neo-ST rats (**C**, **D**). BDA-labeled fibers are observed in the DH on both the ipsilateral and contralateral sides in **A–D**. In the IZ, many BDA-labeled fibers are observed in the ipsilateral dorsal commissural nucleus (arrowhead) in **A–D**. Whereas no BDA-positive projections to the ipsilateral IML are observed in **A** and **B**, BDA-labeled fibers run in the ipsilateral lateral collateral projections to the IML in **C**. In **D**, many BDA-labeled fibers cross the midline to project to the contralateral targets in the DH. **E:** Higher magnification image of the left boxed area in **C**. BDA-labeled fibers make terminal buttons in the IML (box with dotted line). Asterisks: central canal. Scale bars = 100 μm in **A–D**, and 50 μm in E.

Keyence, Osaka, Japan) and transferred to Photoshop CS6 to generate the figures. Some sections were also examined by confocal laser scanning microscopy (FV 1000D; Olympus, Tokyo, Japan) to construct the 3D images. The number of BDA-positive and BDA/CGRP double-positive DRG neurons of intact P40 (n = 4) were counted, and the percentage and standard deviation of BDA/CGRP double-positive neurons per BDA-positive DRG neuron were calculated. The percentage and standard deviation of BDA/RT-97 double-positive neurons per BDA-positive DRG neuron were calculated in the same manner. Histological analysis was performed in four animals of each group.

The cytoarchitecture of the L6 segment was determined by referring to a spinal cord atlas (Sengul et al., 2013). We identified the IML by referring to the results of the retrograde tracing study, as well as to the atlas showing ChAT immunoreactivity in the spinal cord (Nadelhaft and Booth, 1984; Sengul et al., 2013). Although BDA-positive primary afferent fibers projected to the ventral horn, we analyzed the projections to the dorsal horn (DH), and intermediate zone (IZ).

3. Results

3.1. BDA-positive primary afferent fibers in the spinal cord

BDA histochemistry of the spinal cord showed the central projections of BDA-positive primary afferent fibers. In intact rats, BDA-positive fibers projected not only to the ipsilateral spinal cord, but also to the contralateral spinal cord in the L6 segment. Ipsilateral projections were observed in the DH and the IZ. The BDA-labeled fibers, on the other hand, never reached the IML in any section examined. Contralateral projections were observed mainly in the DH (Fig. 1A). The BDA-positive fiber projections in sham-operated rats were similar to those in intact rats (Fig. 1B).

In neo-ST rats, BDA-positive fibers were observed in the DH and IZ of the ipsilateral L6 spinal segment (Fig. 1C, D). Some labeled fibers crossed the midline to project to the ventral part of the DH in the contralateral L6 spinal segment (Fig. 1D). In some sections, the BDA-positive fibers on the ipsilateral side were traced along the lateral edge of the DH, and in the lateral collateral projections to make terminal buttons and varicosities in the ipsilateral IML (Fig. 1E). Projections of BDA-positive fibers to the IML were occasionally observed in serial sections. A double-labeling study for ChAT and BDA showed that BDA-positive varicosities terminated on ChAT-positive neurons in the IML (Fig. 2). These findings suggest that in neo-ST rats, primary afferent fibers originating from L6 DRG neurons project directly to PPNs.

3.2. Chemical markers of DRG neurons with BDA uptake

We examined the chemical markers of DRG neurons that incorporated BDA using immunohistochemistry for RT-97 and CGRP. Many BDA-positive neurons were positive for RT-97 (Fig. 3A–C), and more than half (54.4 ± 12.0%) of the BDA-positive neurons were positive for RT-97. On the other hand, most BDA-positive neurons were negative for CGRP (Fig. 3D–F), and less than 2% (1.8 ± 1.4%) of the BDA-positive neurons were positive for CGRP.

4. Discussion

4.1. Functional recovery

The PPNs in rats are located in the IML region of the L6-S1 spinal segments. The PPNs receive descending projections from several nuclei in the brainstem and hypothalamus (Tang et al., 1998; Puder and Papka 2001a,b). Disruption of these descending projections by complete transection in neo-ST rats might lead to pelvic organ dysfunction. Urinary dysfunction, however, such as anuria, has not been observed. The spinalized rats are able to urinate by themselves. These findings suggest that the spinal cord below the level of transection functions as a micturition center in neo-ST rats.

4.2. De novo ***primary afferent projections to the IML in neo-ST***

In intact and sham-operated rats, no BDA-positive fibers were observed in the IML region in the L6 segment. In neo-ST rats, however, BDA-positive fibers were observed in the IML in the L6 segment on the ipsilateral side, suggesting that SCI at the neona-

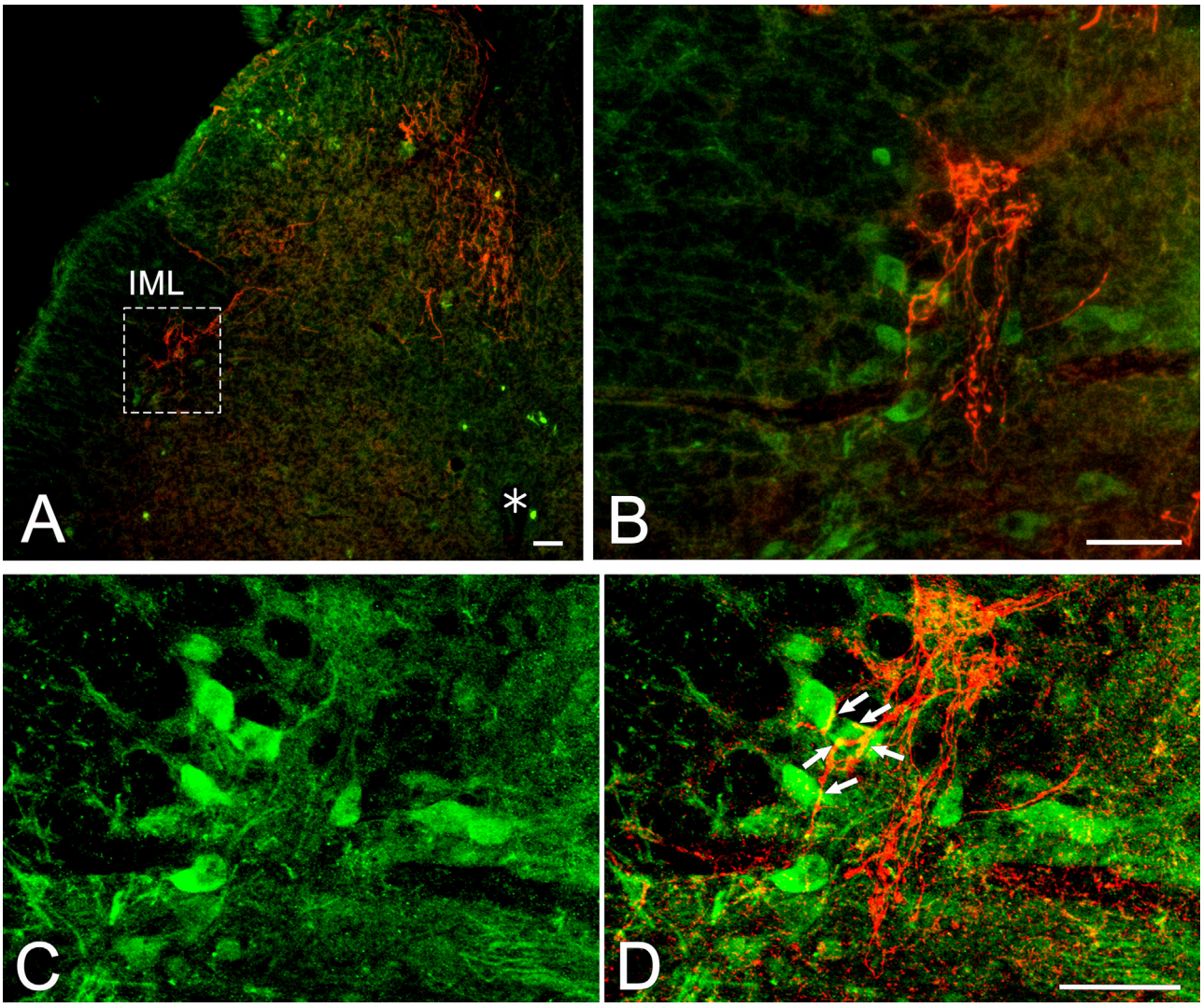

Fig. 2. Double-fluorescence images for ChAT and BDA in the ipsilateral IML of neo-ST rats. **A:** Low-magnification z-stack images of the dorsal spinal cord. BDA-labeled fibers run in the ipsilateral lateral collateral projections to the IML (box with dotted line). **B:** Higher magnification image shows many BDA-positive fibers (red) in the IML containing ChAT-positive neurons (green). **C:** Confocal image of the same section of **B**. Many ChAT-positive neurons are observed. **D:** Double-fluorescence confocal image shows BDA-positive varicosities terminating on ChAT-positive neurons (arrows). Asterisk: central canal. Scale bars = 50 μm in **A–D**. (For interpretation of the references to colour in this figure legend, the reader is referred to the web version of this article.)

tal stage induces plastic changes in BDA-positive fiber projections, particularly *de novo* projections to the IML.

In this study, BDA-positive fibers crossed the midline to project heavily to contralateral targets following neo-ST. In normal cats and rats, sacral primary afferents project to the ventral part of the contralateral DH (Matsushita and Tanami, 1983). Therefore, the present results also suggest that contralateral projections of the L6 primary afferents to the DH were strengthened by neo-ST.

The present double-labeling study showed BDA-positive fibers terminating on cholinergic neurons in the IML, suggesting direct primary afferent projections to PPN cell bodies. Axo-somatic projections, however, are not the only type of projection to active PPNs. The PPNs send dendrites into the dorsal commissure, and to the lateral funiculus and lateral horn of the spinal cord (Nadelhaft and Booth, 1984). We also observed BDA-positive fibers in these dendritic areas of the PPNs in neo-ST rats.

4.3. Characteristics of DRG neurons incorporating BDA

BDA is an anterograde tracer that produces sensitive and detailed labeling of axons and nerve terminals (Reiner and Honig, 2006). The efficiency of BDA for labeling the central projections of primary afferents in comparison with other tracers has been confirmed (Novikov, 2001). On the other hand, BDA injected into the DRG labels only one-third of the DRG neurons (Novikov, 2001). In the present study, many BDA-labeled neurons were RT97-positive, and less than 2% were CGRP-positive in the L6 DRG, suggesting that BDA tends to be incorporated more in neurons with myelinated fibers than in those with unmyelinated fibers containing neuropeptides. Therefore, most of the BDA-labeled fibers in the spinal cord in the present study were considered to comprise myelinated fibers, with few unmyelinated fibers containing neuropeptides. The BDA-labeled fibers projecting to the IML in neo-ST rats are

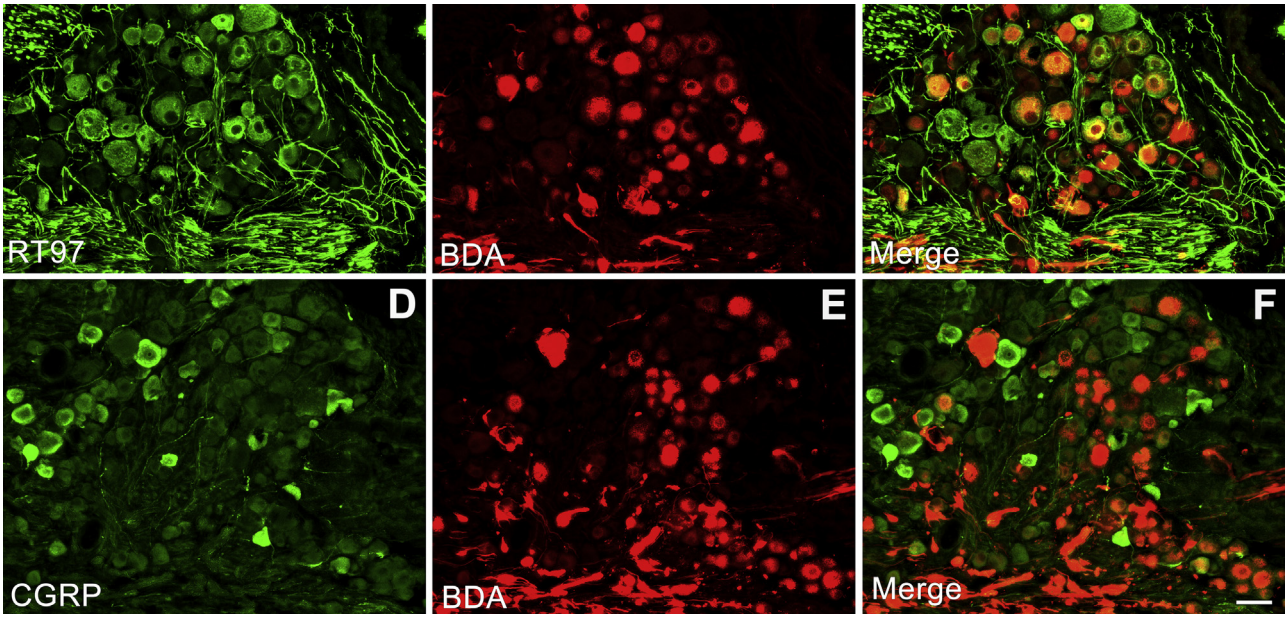

Fig. 3. Double-fluorescence images of DRG sections. **A-C A:** Neurons immunoreactive for RT97 (green); **B:** Fluorescence-labeled BDA-positive neurons (red); **C:** Merged image of **A** and **B**. Many neurons are double-positive for RT97 and BDA. **D-F D:** Neuronal immunohistochemistry for CGRP (green); **E:** Fluorescence-labeled BDA-positive neurons (red); **F:** Merged image of **D** and **E**. Scale bars = 50 μm in **A-F**. (For interpretation of the references to colour in this figure legend, the reader is referred to the web version of this article.)

also considered to be mostly myelinated. Some CGRP-positive primary afferents reportedly project to the IML in neonatal mouse (Funakoshi et al., 2003). It is possible that such projections are also present in rats but not labeled by BDA histochemistry, because BDA was not incorporated by most of the CGRP-positive DRG neurons.

4.4. Functional significance of primary afferent projections to the IML

The L6 dorsal root nerve contains the visceral afferents of both myelinated and unmyelinated fibers from the urinary bladder, as well as somatic afferents from the skeletal muscles associated with the pelvic organs. In the bladder, myelinated Aδ-fibers respond to passive distension and active contraction, whereas unmyelinated C-fibers are not sensitive to bladder filling under physiologic conditions and respond to noxious stimuli, such as chemical irritation or cooling (Fowler et al., 2008). Although myelinated A-fibers comprise only one-third of the bladder afferents in the rat, the normal micturition reflex is principally mediated by A-fiber afferents and the spinobulbospinal pathway via the pontine micturition center in the rat, as well as in the cat (de Groat et al., 1981, 1998; de Groat and Yoshimura, 2010).

Direct primary afferent projections to the PPNs are present, however, in rodents. These projections, which form in the prenatal stage in mouse and contain the neuropeptides CGRP and substance P, and transient receptor potential vanilloid receptor 1 (TRPV1), are speculated to function in the prenatal spinal micturition reflex (Funakoshi et al., 2003, 2006). In animals with spinal injuries that interrupt normal reflex pathways in the adult, the spinal reflex is activated through direct primary afferent projections to the PPNs, which leads to uncontrolled voiding (de Groat et al., 1998; de Groat and Yoshimura, 2010). This spinal micturition reflex is thought to be principally mediated by unmyelinated primary afferents (Krenz and Weaver, 1998; Wang et al., 1998; Zinck et al., 2007) positive for CGRP, substance P, and TRPV1 (de Groat and Yoshimura, 2010). Although sprouting of primary afferents positive for the neurochemical markers CGRP and isolectin B4 might contribute to the recovery of bladder control (Zinck et al., 2007; Zinck and Downie, 2008), later hyperexcitability of unmyelinated primary afferents makes bladder reflexes hyperreflexive (Yoshimura, 1999).

In contrast, the present study suggests that *de novo* projections of myelinated afferents to the PPNs emerged following neo-ST. Myelinated bladder afferent fibers are activated at lower pressure thresholds than unmyelinated fibers (de Groat and Yoshimura, 2010). Therefore, these findings raise the possibility that plastic changes of myelinated fiber projections significantly contribute to the recovery of micturition control following SCI in the neonatal stage.

Acknowledgement

We are grateful to Dr. T. Kadota, Dr. Y. Atobe, Dr. A. Takeda, and Mrs. M. Kobayashi for their expert advice. This work is supported by the fundamental research funding of Yokohama City University.

References

Fowler, C.J., Griffiths, D., de Groat, W.C., 2008. The neural control of micturition. Nat. Neurosci. 9, 453–466.
Funakoshi, K., Goris, R.C., Kadota, T., Atobe, Y., Nakano, M., Kishida, R., 2003. Prenatal development of peptidergic primary afferent projections to mouse lumbosacral autonomic preganglionic cell columns. Dev. Brain Res. 144, 107–119.
Funakoshi, K., Nakano, M., Atobe, Y., Kadota, T., Goris, R.C., 2006. Prenatal development of transient receptor potential vanilloid 1-expressing primary sensory projections to sacral autonomic preganglionic neurons. Neurosci. Lett. 407, 230–233.
Herrera, J.J., Haywood-Watson, R.J.L.I.I., Grill, R.J., 2010. Acute and chronic deficits in the urinary bladder after spinal contusion injury in the adult rat. J. Neurotrauma 27, 423–431.
Krassioukov, A.V., Karlsson, A.K., Wecht, J.M., Wuermser, L.A., Mathias, C.J., Marino, R.J., 2007. Assessment of autonomic dysfunction following spinal cord injury: rationale for additions to International Standards for Neurological Assessment. J. Rehabil. Res. Dev. 44, 103–112.
Krenz, N.R., Weaver, L.C., 1998. Sprouting of primary afferent fibers after spinal cord transection in the rat. Neuroscience 85, 443–458.
Mathias, C.J., Low, D.A., 2014. Autonomic dysfunction. In: Selzer, M.E., et al. (Eds.), Textbook of Neural Repair and Rehabilitation, vol 2. Cambridge University Press, Cambridge, pp. 415–436.
Matsushita, M., Tanami, T., 1983. Contralateral termination of primary afferent axons in the sacral and caudal segments of the cat, as studied by anterograde transport of horseradish peroxidase. J. Comp. Neurol. 220, 206–218.

Nadelhaft, I., Booth, A.M., 1984. The location and morphology of preganglionic neurons and the distribution of visceral afferents from the rat pelvic nerve: a horseradish peroxidase study. J. Comp. Neurol. 226, 238–245.
Novikov, L.N., 2001. Labeling of central projections of primary afferents in adult rats: a comparison between biotinylated dextran amine, neurobiotin™ and *phaseolus vulgaris*-leucoagglutinin. J. Neuosci. Method 112, 145–154.
Puder, B.A., Papka, R.E., 2001a. Hypothalamic paraventricular axons projecting to the female rat lumbosacral spinal cord contain oxytocin immunoreactivity. J. Neurosci. Res. 64, 53–60.
Puder, B.A., Papka, R.E., 2001b. Distribution and origin of corticotropin-releasing factor-immunoreactive axons in the female rat lumbosacral spinal cord. J. Neurosci. Res. 66, 1217–1225.
Reiner, A., Honig, M.G., 2006. Dextran amines: versatile tools for anterograde and retrograde studies of nervous system connectivity. In: Zaborszky, L., Wouterlood, F.G., Lanciego, J.L. (Eds.), Neuroanatomical Tract-Tracing 3. Springer Science + Business Media Inc., New York, pp. 304–335.
Sengul, G., Watson, C., Tanaka, I., Paxinos, G., 2013. Atlas of the Spinal Cord of the Rat, Mouse, Marmoset, Rhesus, and Human. Academic Press, San Diego, pp. 70–75.
Stelzner, D.J., Ershler, W.B., Weber, E.D., 1975. Effects of spinal transection in neonatal and weanling rats: survival of function. Exp. Neurol. 46, 156–177.
Sugaya, K., Roppolo, J.R., Yoshimura, N., Card, J.P., de Groat, W.C., 1997. The central neural pathways involved in micturition in the neonatal rat as revealed by the injection of pseudorabies virus into the urinary bladder. Neurosci. Lett. 223, 197–200.
Takiguchi, M., Atobe, Y., Kadota, T., Funakoshi, K., 2015. Compensatory projections of primary sensory fibers in lumbar spinal cord after neonatal thoracic spinal transection in rats. Neuroscience 304, 349–354.
Tang, Y., Rampin, O., Calas, A., Facchinetti, P., Giuliano, F., 1998. Oxytocinergic and serotonergic innervation of identified lumbosacral nuclei controlling penile erection in the male rat. Neuroscience 82, 241–254.
Wang, H.F., Shortland, P., Park, M.J., Grant, G., 1998. Retrograde and transganglionic transport of horseradish peroxidase-conjugated cholera toxins B subunit, wheatgerm agglutinin and isolectin B4 from *Griffonia simplicifolia* I in primary afferent neurons innervating the rat urinary bladder. Neuroscience 87, 275–288.
Yoshimura, N., 1999. Bladder afferent pathway and spinal cord injury: possible mechanisms inducing hyperreflexia of the urinary bladder. Prog. Neurobiol. 57, 583–606.
Yuan, Q., Su, H., Chiu, K., Wu, W., Lin, Z., 2013. Contrasting neuropathology and functional recovery after spinal cord injury in developing and adult rats. Neurosci. Bull. 29, 509–516.
Zinck, N.D.T., Downie, J.W., 2008. IB4 afferent sprouting contributes to bladder dysfunction in spinal rats. Exp. Neurol. 213, 293–302.
Zinck, N.D.T., Rafuse, V.F., Downie, J.W., 2007. Sprouting of CGRP primary afferents in lumbosacral spinal cord precedes emergence of bladder activity after spinal injury. Exp. Neurol. 204, 777–790.
de Groat, W.C., Yoshimura, N., 2010. Changes in afferent activity after spinal cord injury. Neurol. Urodyn. 29, 63–76.
de Groat, W.C., Nadelhaft, I., Milne, R.J., Booth, A.M., Morgan, C., Thor, K., 1981. Organization of the sacral parasympathetic reflex pathways to the urinary bladder and large intestine. J. Auton. Nerv. Syst. 3, 135–160.
de Groat, W.C., Araki, I., Vizzard, M.A., Yoshiyama, M., Yoshimura, N., Sugaya, K., Tai, C., Roppolo, J.R., 1998. Developmental and injury induced plasticity in the micturition reflex pathway. Behav. Brain Res. 92, 127–140.